



Article

In Vivo Inhibition of TRPC6 by SH045 Attenuates Renal Fibrosis in a New Zealand Obese (NZO) Mouse Model of Metabolic Syndrome

Zhihuang Zheng ^{1,2} , Yao Xu ³, Ute Krügel ⁴ , Michael Schaefer ⁴, Tilman Grune ^{5,6}, Bernd Nürnberg ⁷ , May-Britt Köhler ², Maik Gollasch ^{1,3,*}, Dmitry Tsvetkov ^{3,*} and Lajos Markó ^{2,6,8,9,*}

- ¹ Department of Nephrology/Intensive Care, Charité—Universitätsmedizin Berlin, Corporate Member of Freie Universität Berlin and Humboldt-Universität zu Berlin, 10117 Berlin, Germany; zhihuang.zheng@charite.de
- ² Experimental and Clinical Research Center, a Joint Cooperation of the Charité—University Medicine Berlin and Max Delbrück Center for Molecular Medicine in the Helmholtz Association, 13125 Berlin, Germany; may-britt.koehler@charite.de
- ³ Department of Internal Medicine and Geriatrics, University Medicine Greifswald, 17475 Greifswald, Germany; yao.xu@med.uni-greifswald.de
- ⁴ Rudolf Boehm Institute for Pharmacology and Toxicology, Leipzig University, 04107 Leipzig, Germany; ute.kruegel@medizin.uni-leipzig.de (U.K.); michael.schaefer@medizin.uni-leipzig.de (M.S.)
- ⁵ Department of Molecular Toxicology, German Institute of Human Nutrition Potsdam-Rehbruecke (DIfE), 14558 Nuthetal, Germany; tilman.grune@dife.de
- ⁶ DZHK (German Centre for Cardiovascular Research), Partner Site, 10785 Berlin, Germany
- ⁷ Department of Pharmacology, Experimental Therapy and Toxicology and Interfaculty Center of Pharmacogenomics and Drug Research, University of Tübingen, 72076 Tübingen, Germany; bernd.nuernberg@uni-tuebingen.de
- ⁸ Berlin Institute of Health at Charité—Universitätsmedizin Berlin, 10178 Berlin, Germany
- ⁹ Charité—Universitätsmedizin Berlin, Corporate Member of Freie Universität Berlin and Humboldt-Universität zu Berlin, 10117 Berlin, Germany
- * Correspondence: maik.gollasch@med.uni-greifswald.de (M.G.); dmitry.tsvetkov@med.uni-greifswald.de (D.T.); lajos.marko@charite.de (L.M.)



Citation: Zheng, Z.; Xu, Y.; Krügel, U.; Schaefer, M.; Grune, T.; Nürnberg, B.; Köhler, M.-B.; Gollasch, M.; Tsvetkov, D.; Markó, L. In Vivo Inhibition of TRPC6 by SH045

Attenuates Renal Fibrosis in a New Zealand Obese (NZO) Mouse Model of Metabolic Syndrome. *Int. J. Mol. Sci.* **2022**, *23*, 6870. <https://doi.org/10.3390/ijms23126870>

Academic Editors: Luís Belo and Márcia Carvalho

Received: 18 March 2022

Accepted: 16 June 2022

Published: 20 June 2022

Publisher's Note: MDPI stays neutral with regard to jurisdictional claims in published maps and institutional affiliations.



Copyright: © 2022 by the authors. Licensee MDPI, Basel, Switzerland. This article is an open access article distributed under the terms and conditions of the Creative Commons Attribution (CC BY) license (<https://creativecommons.org/licenses/by/4.0/>).

Abstract: Metabolic syndrome is a significant worldwide public health challenge and is inextricably linked to adverse renal and cardiovascular outcomes. The inhibition of the transient receptor potential cation channel subfamily C member 6 (TRPC6) has been found to ameliorate renal outcomes in the unilateral ureteral obstruction (UUO) of accelerated renal fibrosis. Therefore, the pharmacological inhibition of TRPC6 could be a promising therapeutic intervention in the progressive tubulo-interstitial fibrosis in hypertension and metabolic syndrome. In the present study, we hypothesized that the novel selective TRPC6 inhibitor SH045 (larixyl N-methylcarbamate) ameliorates UUO-accelerated renal fibrosis in a New Zealand obese (NZO) mouse model, which is a polygenic model of metabolic syndrome. The in vivo inhibition of TRPC6 by SH045 markedly decreased the mRNA expression of pro-fibrotic markers (*Col1a1*, *Col3a1*, *Col4a1*, *Acta2*, *Ccn2*, *Fn1*) and chemokines (*Cxcl1*, *Ccl5*, *Ccr2*) in UUO kidneys of NZO mice compared to kidneys of vehicle-treated animals. Renal expressions of intercellular adhesion molecule 1 (ICAM-1) and α -smooth muscle actin (α -SMA) were diminished in SH045- versus vehicle-treated UUO mice. Furthermore, renal inflammatory cell infiltration (F4/80+ and CD4+) and tubulointerstitial fibrosis (Sirius red and fibronectin staining) were ameliorated in SH045-treated NZO mice. We conclude that the pharmacological inhibition of TRPC6 might be a promising antifibrotic therapeutic method to treat progressive tubulo-interstitial fibrosis in hypertension and metabolic syndrome.

Keywords: TRPC6; UUO; NZO mice; inflammation; fibrosis; CKD; SH045

1. Introduction

Chronic kidney disease (CKD) is characterized by progressive loss of kidney function. The main risk factors of developing CKD are the combination of obesity, diabetes and hypertension, which is commonly referred to as metabolic syndrome. Other contributors are autoimmune diseases (e.g., glomerulonephritis), environmental exposures and genetic risk factors [1,2]. Morphologically, persistent low-grade renal inflammation and tubulointerstitial fibrosis are key hallmarks of CKD [3,4]. The complex interplay of fibroblasts, lymphocytes, tubular, and other cell types in the kidney lead to excessive extracellular matrix deposition and the further deterioration of renal function [5,6]. Although unspecific treatments strategies are available (e.g., medications lowering blood pressure), CKD progression is still poorly controlled.

In recent years, novel drug targets, such as transient receptor potential cation channel, subfamily C, and member 6 (TRPC6), emerged [7,8]. *TRPC6* mutations lead to glomerular injury and proteinuria, presumably involving the Ca^{2+} signaling pathway and resulting in progressive kidney failure [9–12]. Both *TRPC6* gain-of-function and loss-of-function cause familial forms of focal segmental glomerulosclerosis (FSGS) [11,13]. Interestingly, in a murine model of kidney injury (unilateral ureteral obstruction (UUO)), *Trpc6*^{-/-} deficiency and pharmacological blockade with BI-749327 ameliorated renal fibrosis in C57BL/6J mice [7,8]. Remarkably, these beneficial effects were not observed in the acute stage of kidney injury (AKI) [14]. Thus, *TRPC6* inhibition may have effects on renal fibrogenesis during AKI-to-CKD transition. Given this state of affairs, *TRPC6* inhibition seems to represent a promising new therapeutic approach to combat progressive renal failure since it potentially affects CKD at later stages after kidney injury. However, it is unknown whether *TRPC6* inhibition is effective for inhibiting progressive tubulo-interstitial fibrosis in hypertension and metabolic syndrome.

Recently, by the chemical diversification of (+)-larixol originating from *Larix decidua* resin traditionally used for inhalation, its methylcarbamate congener, named SH045, was developed as a novel, highly potent, subtype-selective inhibitor of *TRPC6* [15]. In the present study, we hypothesized that this novel selective *TRPC6* inhibitor (SH045) [15] could ameliorate renal fibrogenesis in the New Zealand obese (NZO) mouse model, which is a polygenic model of metabolic syndrome [16]. We studied the therapeutic effects of the in vivo inhibition of *TRPC6* by the novel blocker SH045 in the UUO mouse model of accelerated renal fibrogenesis utilizing these mice.

2. Results

2.1. SH045 Treatment Does Not Affect Renal Function and *Trpc* Expression in UUO Model

To investigate the impact of in vivo *TRPC6* inhibition on renal function, target molecules and fibrosis, we performed UUO in the NZO mice. During the one week period, we administered SH045 (*TRPC6* inhibitor) or vehicle once daily (Figure 1A). After 7 days, urinary tract obstruction led to hydronephrosis (Figure S1). Consistent with our previous findings, *Trpc6* expression significantly increased in UUO kidneys. SH045 affected neither *Trpc6* mRNA expression nor the expression of other *TRPC* channels, including *Trpc1*, *Trpc2*, *Trpc3* and *Trpc4* (Figure 1B and Figure S2A–D). SH045 had no impact on renal function. Serum creatinine ($p = 0.1098$; Figure 1B) and blood urea nitrogen (BUN) ($p = 0.928$; Figure 1C), serum cystatin C, urine albumin, and urine albumin-to-creatinine ratio in SH045-treated mice were unchanged (Figure 1D–F). In addition, we found no differences in serum levels of glucose, sodium, potassium, ionized calcium, total CO_2 , hemoglobin, hematocrit, and anion gap in SH045-treated animals compared to the vehicle group (Table S1). SH045-treated mice exhibited a slightly higher serum chloride concentration ($p = 0.047$), albeit within the normal physiological range.

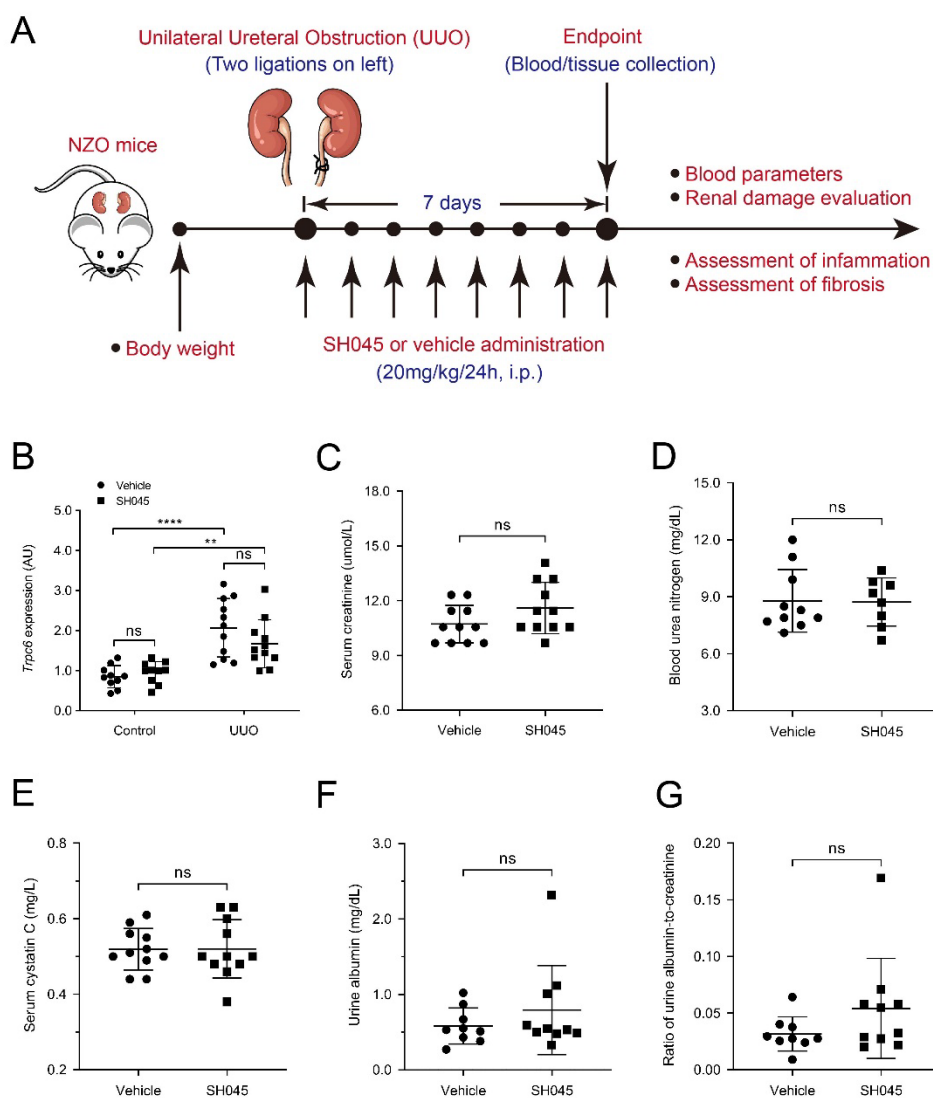


Figure 1. Impact of SH045 administration on renal function and *Trpc6* expression in UUO model. (A) Experimental design of unilateral ureteral obstruction (UUO) model. NZO mice were subjected to UUO and then injected with SH045 ($n = 11$) or vehicle ($n = 11$) once every 24 h between day 0 and day 7. All mice were euthanized on day 7 after UUO surgery. (B) Renal mRNA levels of *Trpc6* (control $n = 10$, UUO $n = 11$). Control group includes kidneys that were not subjected to the UUO. (C) Serum levels of creatinine, (D) blood urea nitrogen, and (E) cystatin C in the experimental UUO groups. (F) Urine albumin and (G) ratio of albumin to creatinine in the experimental UUO groups (UUO vehicle $n = 10$ – 11 , UUO SH045 $n = 8$ – 11). Data expressed as means \pm SD. Two-way ANOVA followed by Sidak's multiple comparisons post hoc test. ** $p < 0.01$ and **** $p < 0.0001$ defined as significant. ns, not statistically significant. AU, arbitrary units.

2.2. SH045 Treatment Does Not Alter Kidney Parenchymal Damage

Morphologically, UUO increased mesangial matrix deposition, leading to glomerular hypertrophy, and tubular dilatation (Figure 2A–D). The expressions of renal damage markers, kidney injury molecule-1 (*Havcr1*) and Lipocalin-2 (*Lcn2*), were increased in UUO kidneys compared to control (Figure 2E,F). However, SH045 did not affect these parameters in both UUO and control kidneys (Figure 2A–F). These results indicate that TRPC6 inhibition per se has no impact on the damage to renal parenchyma (glomerular or tubular) caused by UUO.

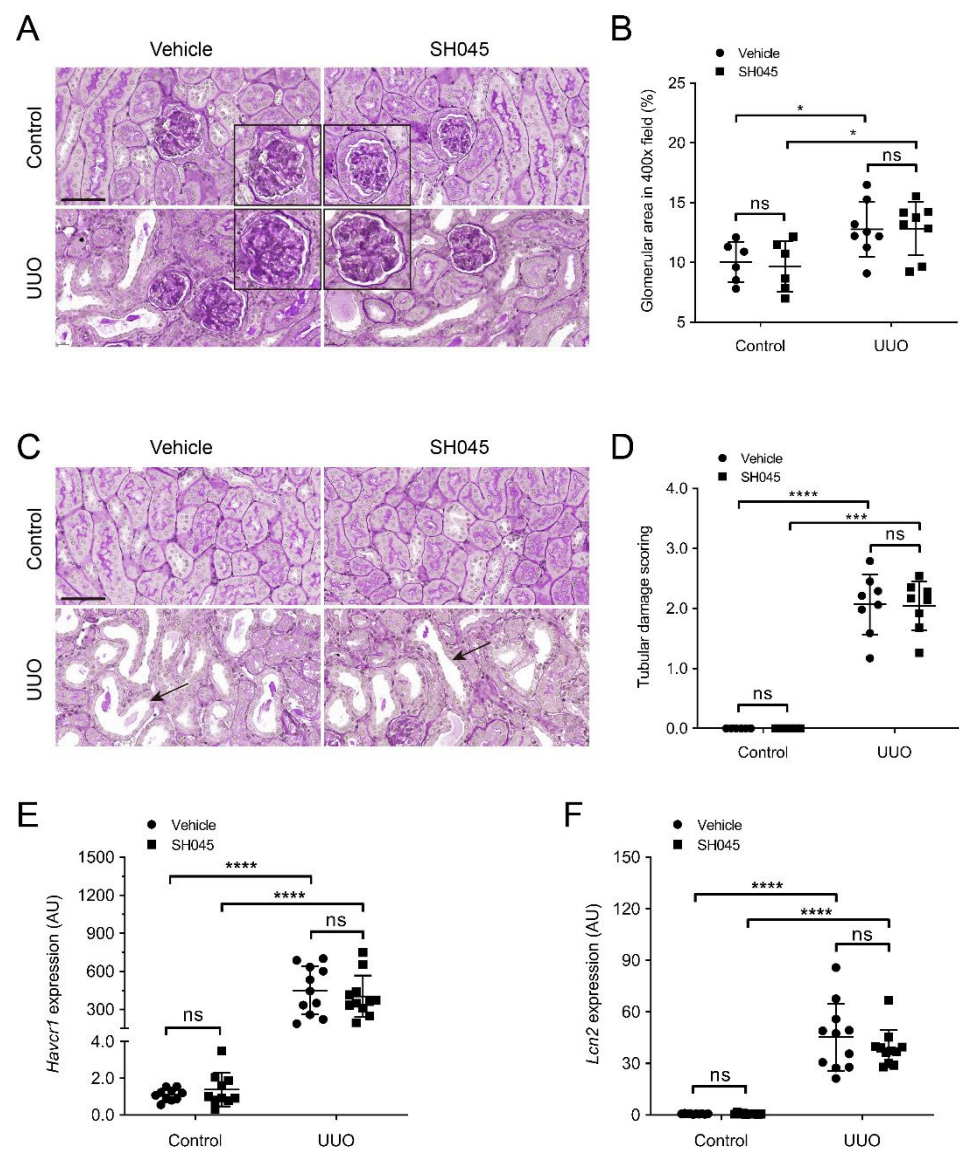


Figure 2. SH045 impact on kidney histopathology after UUO. (A) Representative images of UUO-injured glomerulus (magnification: 400 \times). Kidney sections were stained with periodic acid–Schiff staining (PAS). (B) Quantification of glomerular damage (control $n = 6$, UUO $n = 8$). (C) Representative images of UUO-injured tubules (magnification: 400 \times). Kidneys sections were stained with periodic acid–Schiff staining (PAS). Arrows indicate tubular injury. Scale bars are 50 μm . (D) Semi-quantification of tubular damage (control $n = 6$, UUO $n = 8$). (E) Renal mRNA levels of kidney injury molecule 1 (*Havcr1*) and (F) Lipocalin 2 (*Lcn2*) (control $n = 10$, UUO $n = 11$). Data expressed as means \pm SD. Two-way ANOVA followed by Sidak’s multiple comparisons post hoc test. * $p < 0.05$, *** $p < 0.001$ and **** $p < 0.0001$ defined as significant. ns, not statistically significant. AU, arbitrary units.

2.3. SH045 Treatment Ameliorates Renal Expression of Inflammatory Markers

Next, we measured the renal mRNA expression of inflammatory cytokines and chemokines using qRT-PCR. The expression of inflammatory molecules was markedly increased in kidneys subjected to UUO compared to control groups (Figure 3). The mRNA expression of chemokine (C-X-C motif) ligand 1 (*Cxcl1*), chemokine (C-C motif) ligand 5 (*Ccl5*), and chemokine (C-C motif) receptor 2 (*Ccr2*) was significantly lower in UUO kidneys of SH045-treated mice (SH045 UUO kidneys) compared to UUO kidneys of vehicle-treated mice (vehicle UUO kidneys) (Figure 3A–C). The expressions of chemokine (C-C

motif) ligand 2 (*Ccl2*), chemokine (C-X-C motif) ligand 2 (*Cxcl2*), and intercellular adhesion molecule 1 (*Icam1*) were increased in both SH045 UUO and vehicle UUO kidneys compared to control kidneys, although there were no differences between SH045 UUO and vehicle UUO kidneys ($p = 0.056$, $p = 0.068$ and $p = 0.076$, respectively) (Figure 3D–F). Furthermore, immunofluorescence staining of ICAM-1 markedly increased in UUO kidneys in comparison to control kidneys (Figure S3A–C). Additionally, the pharmacological inhibition of TRPC6 by SH045 decreased ICAM-1 expression after UUO in comparison to vehicle-treated kidneys (Figure S3A–C). Whereas ICAM1 expression was similar in the vessels of UUO kidneys, vehicle-treated kidneys had a much higher expression in SH045-treated UUO kidneys due to more ICAM-1-positive immune cell infiltration (Figure S3A).

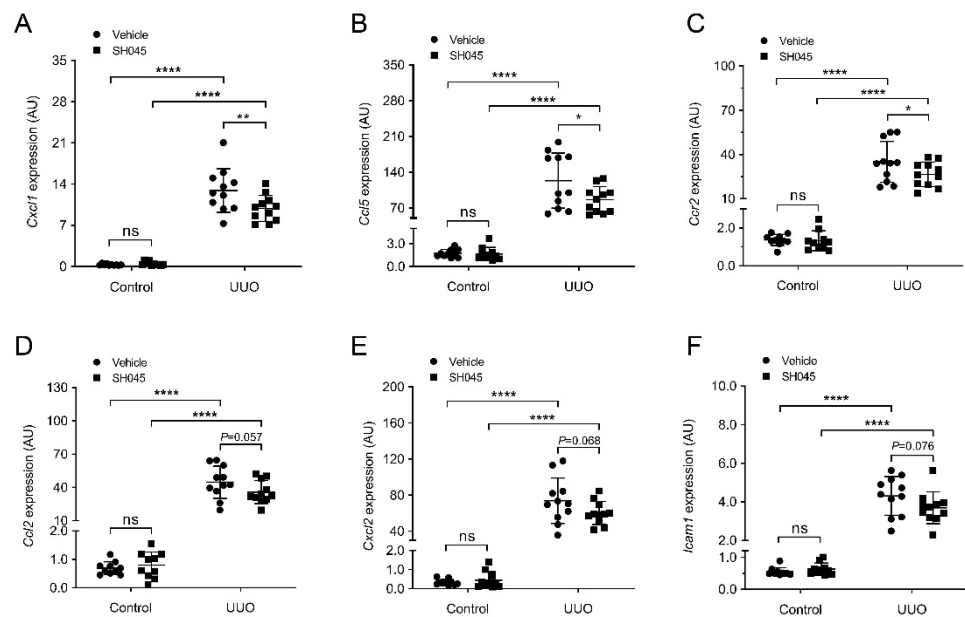


Figure 3. SH045 impact on renal expression of inflammatory markers. (A) Renal mRNA levels of chemokine (C-X-C motif) ligand 1 (*Cxcl1*), (B) chemokine (C-C motif) ligand 5 (*Ccl5*), (C) chemokine (C-C motif) receptor 2 (*Ccr2*), (D) chemokine (C-C motif) ligand 2 (*Ccl2*), (E) chemokine (C-X-C motif) ligand 2 (*Cxcl2*), and (F) intercellular adhesion molecule-1 (*Icam1*) (control $n = 10$, UUO $n = 11$). Data expressed as means \pm SD. Two-way ANOVA followed by Sidak's multiple comparisons post hoc test. * $p < 0.05$, ** $p < 0.01$, and **** $p < 0.0001$ defined as significant. ns, not statistically significant. AU, arbitrary units.

2.4. SH045 Treatment Leads to Less Renal Immune Cell Infiltration

To evaluate inflammatory cell infiltration in UUO kidneys, we examined macrophages and T cell presence using immunofluorescence. Kidney cross sections were immunolabelled with the macrophage marker F4/80 and T cell marker CD4 as described previously [17]. As shown in Figure 4A,B, excessive CD4-positive cells infiltration was observed in renal interstitium of UUO kidneys in comparison to control kidneys (Figure 4A,B). Similarly, the number of F4/80-positive cells in UUO kidneys was also markedly increased compared to control kidneys (Figure 4C,D). In accordance with ameliorated inflammatory cytokine and chemokine expression, SH045 treatment decreased UUO-induced macrophage and T cell infiltration (Figure 4A–D). Thus, these data suggest that TRPC6 inhibition reduces renal inflammation in the UUO model of NZO mice.

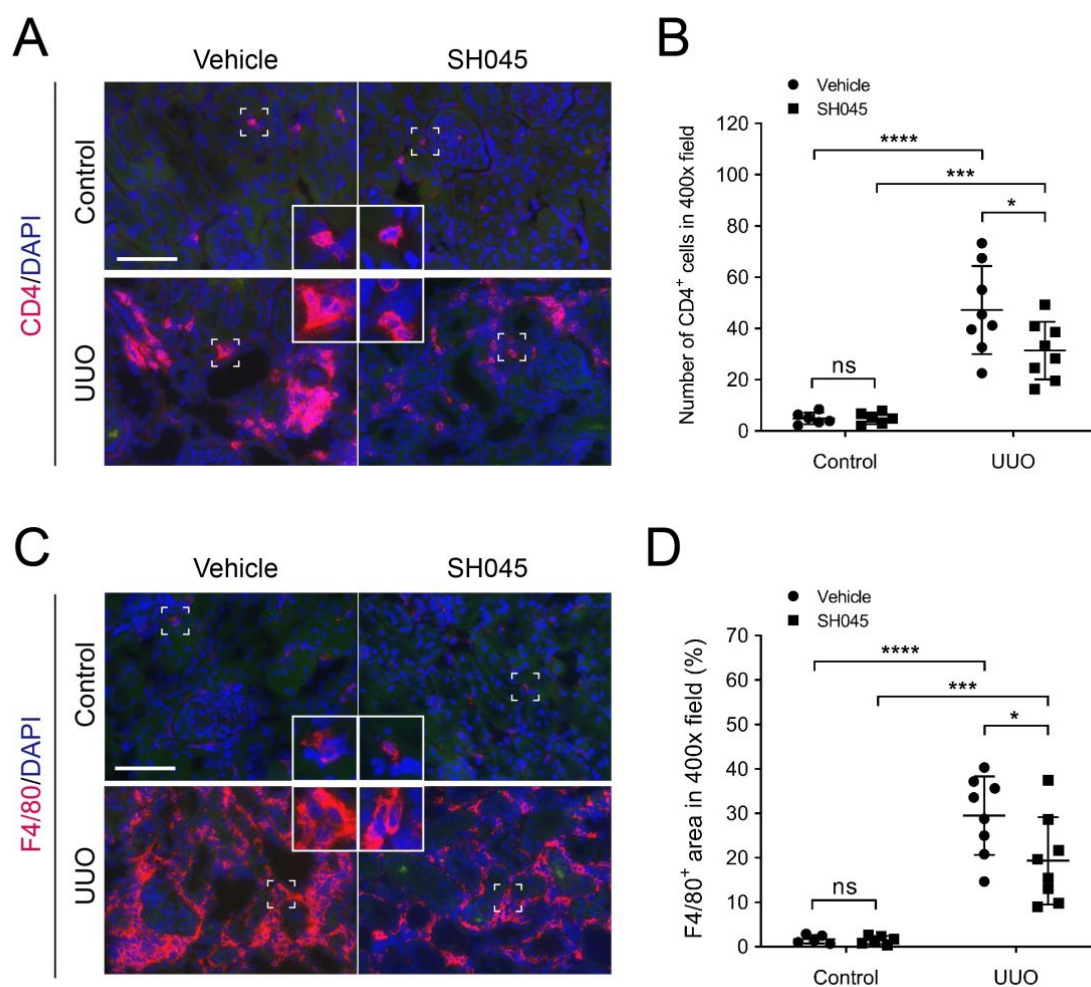


Figure 4. SH045 impact on renal inflammatory cell accumulation after UUO. (A) Representative images of control and UUO-injured kidneys stained with CD4+ T cells (magnification: 400×). Rectangles represent single-cell magnifications. Scale bars are 50 μm. (B) Quantification in renal infiltration of CD4+ T cells (control $n = 6$, UUO $n = 8$). (C) Representative images of control and UUO-injured kidneys stained with F4/80+ macrophages (magnification: 400×). Rectangles represent single-cell magnifications. Scale bars are 50 μm. (D) Quantification in renal infiltration of F4/80+ macrophages (control $n = 6$, UUO $n = 8$). Data expressed as means \pm SD. Two-way ANOVA followed by Sidak's multiple comparisons post hoc test. * $p < 0.05$, *** $p < 0.001$, and **** $p < 0.0001$ defined as significant. ns, not statistically significant. AU, arbitrary units.

2.5. SH045 Treatment Reduces Renal Expression of Fibrotic Markers

Since progressive fibrosis is a typical lesion occurring after UUO [18], we examined the impact of SH045 administration on renal fibrosis. We measured the renal mRNA expression of pro-fibrotic markers, including collagen I (*Col1a2*), collagen III (*Col3a1*), collagen IV (*Col4a3*), α -smooth muscle actin (*Acta2*), connective tissue growth factor (*Ccn2*), and fibronectin (*Fn1*). All these fibrosis-associated genes were upregulated after UUO (Figure 5A–F). Notably, SH045 treatment significantly reduced *Col1a2*, *Col3a1*, *Col4a3*, *Acta2*, *Ccn2*, and *Fn1* expressions in the UUO kidney (Figure 5A–F).

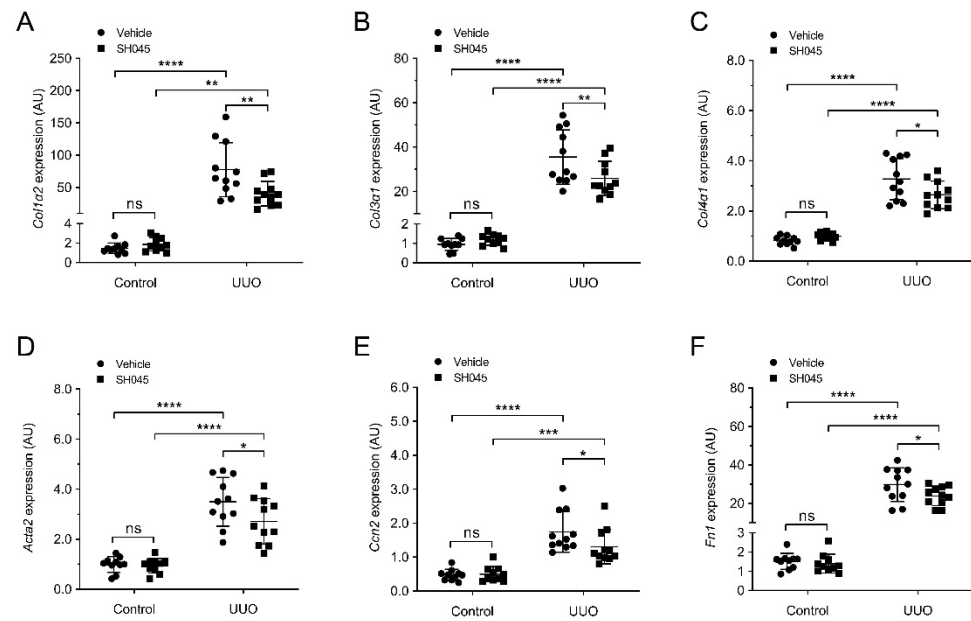


Figure 5. SH045 impact on expression of renal fibrotic markers UUO. (A) Renal mRNA levels of collagen type I α 1 (*Col1a2*), (B) Collagen type III α 1 (*Col3a1*), (C) Collagen type IV α 1 (*Col4a1*), (D) α -Smooth muscle actin (*Acta2*), (E) Connective tissue growth factor (*Ccn2*), and (F) Fibronectin (*Fn1*) (Control $n = 10$, UUO $n = 11$). Data expressed as means \pm SD. Two-way ANOVA followed by Sidak's multiple comparisons post hoc test. * $p < 0.05$, ** $p < 0.01$, *** $p < 0.001$ and **** $p < 0.0001$ defined as significant. ns, not statistically significant. AU, arbitrary units.

To further confirm our qPCR data, Sirius red (SR) and fibronectin immunofluorescence staining was performed. Control kidneys exhibited small SR-positive (+) areas. In contrast, UUO kidneys displayed markedly increased SR⁺ areas compared to control kidneys, indicating that UUO caused considerable collagen deposition (Figure 6A,B). SH045 effectively decreased this collagen deposition (Figure 6A,B). Similarly, immunofluorescence staining revealed increased fibronectin deposition and chromogenic immunohistochemistry increased α -smooth muscle actin (α -SMA) expression in UUO kidneys in comparison to control kidneys, which were reduced by SH045 treatment (Figure 6C–F). Taken together, these data suggest that renal fibrosis and inflammatory reactions are ameliorated in response to in vivo TRPC6 inhibition by SH045.

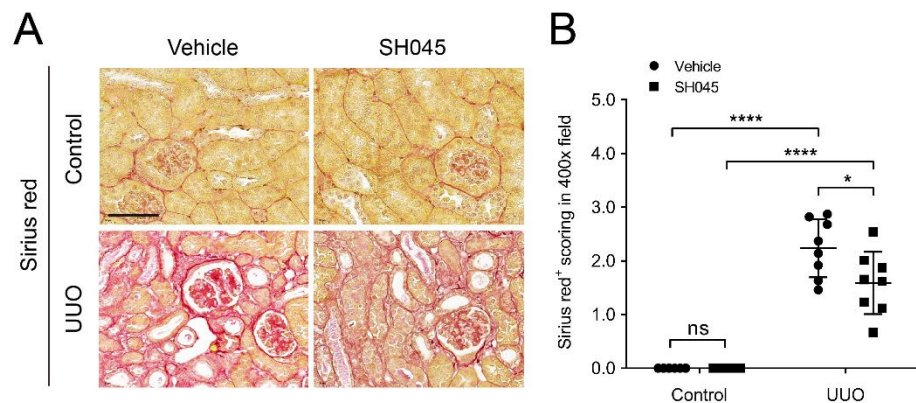


Figure 6. Cont.

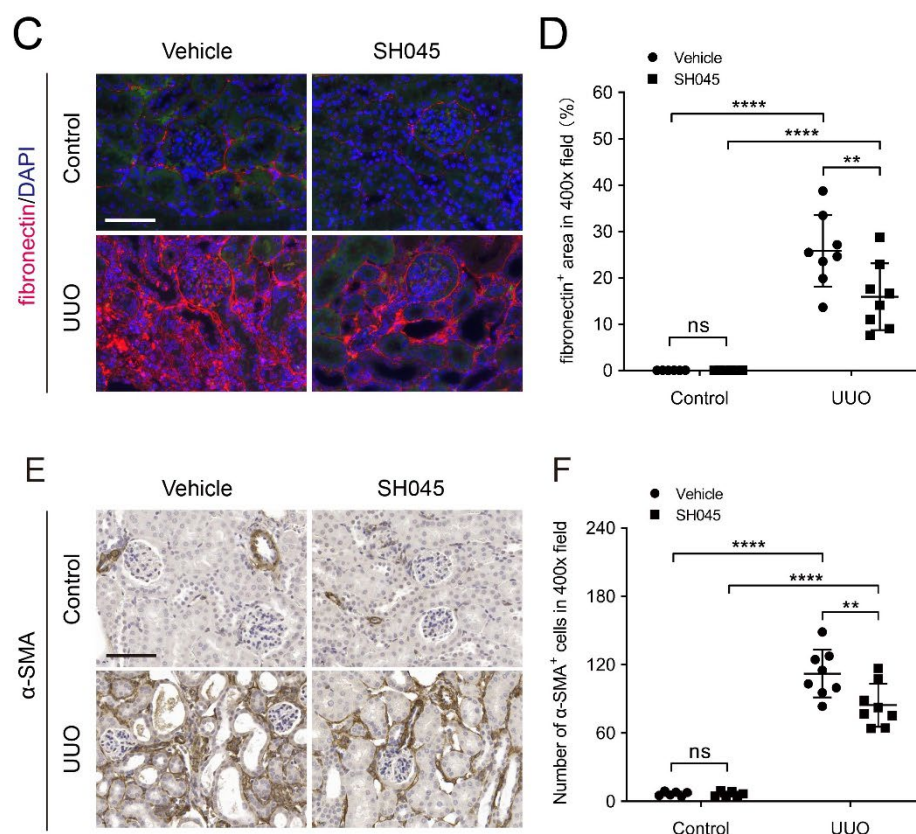


Figure 6. SH045 impact on renal fibrogenesis after UUO. (A) Representative images of control and UUO-injured kidneys stained with Sirius red (magnification: 400 \times). Scale bars are 50 μ m. (B) Semi-quantification in renal Sirius red+ area proportion (control $n = 6$, UUO $n = 8$). (C) Representative images of control and UUO-injured kidneys stained with fibronectin (magnification: 400 \times). Scale bars are 50 μ m. (D) Quantification in fibronectin+ area (control $n = 6$, UUO $n = 8$). (E) Representative images of control and UUO-injured kidneys stained with α -SMA (magnification: 400 \times). Scale bars are 50 μ m. (F) Quantification of α -SMA+ staining (control $n = 6$, UUO $n = 8$). Data expressed as means \pm SD. Two-way ANOVA followed by Sidak's multiple comparisons post hoc test. * $p < 0.05$, ** $p < 0.01$, and **** $p < 0.0001$ defined as significant. ns, not statistically significant.

3. Discussion

Renal fibrosis is the final common outcome of progressive CKD, which is often observed in metabolic syndrome [19]. To date, there are few clinical treatments that successfully target fibrosis in CKD. Thus, developing new drug treatments is the current focus. Increasing evidence indicates that TRPC6 could play a critical role in kidney fibrosis [20]. In our previous study using *Trpc6*^{-/-} mice, we found that TRPC6 deficiency ameliorated renal fibrosis and immune cellular infiltration in the UUO model [7]. However, the results were difficult to interpret due to confounding genomic and non-genomic effects of other TRPC channels, e.g., TPRC1, TRPC3, TRPC4 and TRPC5. Previous studies identified SH045 (larixyl N-methylcarbamate) as a novel, highly potent, subtype-selective inhibitor of TRPC6 channels [15]. In our previous study, we found that the in vivo inhibition of TRPC6 by SH045 had no effects on acute kidney injury (AKI) [14]. However, there are no studies on the effects of SH045 in kidney fibrosis. In the present study, we tested the hypothesis that SH045 ameliorates UUO-accelerated renal fibrosis in NZO mice.

Our results show that SH045 ameliorates fibrotic processes in UUO kidneys. Expressions of all investigated fibrosis or fibrosis-related genes were ameliorated by SH045 treatment. The histological assessment of deposited collagen and extracellular matrix protein confirmed the expression data of the genes. Of note, renal fibrosis arises after an insult, whereas resident kidney fibroblasts and cells of hematopoietic origin differentiate

into myofibroblasts [21–23]. Myofibroblasts acquire a contractile/proliferative phenotype upon activation by profibrotic factors and become principal kidney collagen-producing cells [24]. Considerable evidence indicates that renal inflammation plays a central role in the initiation and progression of fibrosis [19]. Myofibroblasts are regulated by a variety of means, including paracrine signals derived from lymphocytes and macrophages. Critical chemokines recruiting macrophages and lymphocytes are CCL2/CCR2, CCL5, and CXCL1/2. ICAM-1 is an endothelial- and leukocyte-associated transmembrane protein in facilitating leukocyte endothelial transmigration [25]. Interestingly, our results show that SH045 inhibits the overexpression of these chemokines and the infiltration of numerous immune cells, suggesting that TRPC6 inhibition may antagonize renal fibrosis by affecting inflammatory processes. TRPC6 is expressed in a wide range of cell types, including neutrophils, lymphocytes, platelets and the endothelium, which might be a modulator of tissue susceptibility to inflammatory injuries [26,27]. Some studies suggested that TRPC6 channels may enhance chemotactic responses by increasing Ca^{2+} concentration, which promotes actin-based cytoskeleton remodeling [28,29]. Furthermore, Ca^{2+} currents within T-lymphocytes are influenced by TRPC6, which can affect the function of T-lymphocytes [30]. Novel myeloid cell subsets could be targeted to ameliorate injury or enhance repair, including an *Arg1*⁺ monocyte subset present during injury and *Mmp12*⁺ macrophages present during repair [31]. It is intriguing to speculate that TRPC6 inhibition might ameliorate fibrotic processes in UUO kidneys by modulating the function(s) of these cell types.

On the other hand, TRPC6 was also reported to contribute to fibroblast transdifferentiation and healing in vivo [32]. Thus, the beneficial effects of TRPC6 inhibition seen in the UUO model might also involve fibroblasts. A TRPC6 blockade may decrease Ca^{2+} dependent activation of MEK/ERK signaling pathway [33]. Of note, this pathway was implemented in the detrimental differentiation and expansion of kidney fibroblasts [34]. The inhibition of the ERK1/2 pathway by trametinib ameliorated UUO-induced fibrosis through the mammalian target of rapamycin complex 1 (mTORC1) and its downstream targets.

In the present study, SH045 did not affect renal function parameters in 7-day-UUO mice, which is not surprising. In this short-term UUO model, the kidney function of contralateral undamaged kidney remained preserved and compensated for the loss of the obstructed kidney at the early stage [35]. We used the NZO inbred obese mouse strain, which carries susceptibility genes for diabetes and hypertension, conditions similar to metabolic syndrome and CKD in humans [36]. Our data observed in UUO induced fibrosis in NZO mice, and thus might be of importance in mimicking human CKD pathophysiology.

Renal fibrosis involves complex interactions among multiple cells and cytokine signaling pathways. Further studies of the TRPC6 modulation of renal fibrosis using single-cell RNA sequencing could help to better understand the exact mechanism(s) of action in the different cell types. Single-cell RNA sequencing enables the precise discrimination of specific cell type(s) or cell state(s) enriched in certain conditions (e.g., UUO) [31]. Thus, selecting cellular labels based on gene expression markers could represent a novel approach to determine cell type(s) or cell state(s) predominantly influenced by the inhibition of TRPC6 (by SH045) in the UUO model. Understanding the mechanisms behind TRPC6-induced fibrogenesis is essential for developing novel therapies to slow the progression of CKD.

Our study demonstrates that the in vivo administration of SH045 ameliorates immune cell infiltration and fibrosis in NZO mice subjected to UUO, which makes SH045 a promising therapeutic drug strategy in CKD treatment for metabolic syndrome.

4. Materials and Methods

4.1. Animals

Male NZO mice ($n = 22$, NZO/BomHIDife genetic background) from Max-Rubner-Laboratory, German Institute of Human Nutrition Potsdam-Rehbrücke (Nuthetal, Germany) were used. These mice had increased weight (45.90 ± 4.11 g b.w) and were previously characterized [7]. Mice were held in specific-pathogen-free (SPF) condition, in a 12:12 h

light–dark cycle, with free access to food and drinking water. All experimental procedures were approved by the Berlin Animal Review Board, Berlin, Germany and followed the restrictions in the Berlin State Office for Health and Social Affairs (LaGeSo) [37]. All experiments were performed in accordance with ARRIVE guidelines [38].

4.2. UUO Model

UUO mouse model was performed as described earlier [7]. Briefly, NZO mice were anaesthetized by isoflurane (2.2%) supplied with air flow at approximately 350 mL/min. During the surgery mice were placed on a heating pad to prevent hypothermia. Preemptive analgesia with carprofen (5–10 mg/kg b.w) was subcutaneously used. Body temperature was maintained at 37.5 °C and monitored during surgery using a temperature controller with a heating pad (TCAT-2, Physitemp Instruments, Clifton, NJ, USA). In deep anesthesia, the anterior abdominal skin was shaved. Then, a midline laparotomy was conducted via an incision of the avascular linea alba, and the left ureter was exposed from left side. The ureter was then ligated twice close to the renal pelvis using a 5–0 polyglycolic acid (PGA) suture wire (Resorba[®], Nürnberg, Germany). The linea alba and skin were closed separately. The wound was sanitized with a silver aluminium spray (Henry Schein[®], Berlin, Germany), and 0.5 mL of warm (37 °C) isotonic sodium chloride solution was intraperitoneally injected. Subsequently, each mouse was placed in a cage in front of an infrared (IR) lamp and monitored until they recovered consciousness. For the following two days, mice received carprofen (2.5 mg/mL) in their drinking water (1:50) with a final concentration of 0.05 mg/mL. After surgery mice had free access to drinking water and chow. Seven days after UUO surgery, mice were sacrificed by overdose of isoflurane and cervical dislocation. The blood samples were collected for further analysis and left kidneys were removed immediately. The kidneys were divided into three portions. Upper part of the kidney tissue was frozen in isopthane. Middle part of kidney was immersed in 4% phosphate–buffered saline (PBS)-buffered formalin for histological assessment. The other left tissue was snap frozen in liquid nitrogen for RNA preparation.

4.3. TRPC6 Inhibitor

SH045 (Larixyl-6-N-methylcarbamate) was previously described [15]. SH045 was initially dissolved in DMSO (final concentration of DMSO is 0.5%) and then in 5% Cremophor EL[®] solution with 0.9% NaCl and used for intraperitoneal injection (i.p.). Mice subjected to UUO were treated with SH045 (20 mg/kg once per day, i.p.) or vehicle daily until day 7 after surgery.

4.4. Blood Measurements and Drugs

The blood measurements of sodium, potassium, chloride, ionized calcium, total carbon dioxide, glucose, urea nitrogen, creatinine, hematocrit, hemoglobin, and anion gap were performed at endpoint. Nighty-five microliters of blood were taken from the facial vein, and parameters were measured using i-STAT system with Chem8+ cartridges (Abbott GmbH, Wiesbaden, Germany).

4.5. Quantitative Real-Time (qRT)-PCR

The qRT-PCR was performed as previously described [7]. Briefly, total mRNA from mice was isolated from snap–frozen kidneys using RNeasy RNA isolation kit (Qiagen, Australia), according to the manufacturer’s instructions. The concentration and quality of RNA were determined by NanoDrop-1000 spectrophotometer (Thermo Fisher Scientific, Waltham, MA, USA). Next, RNA was transcribed to cDNA using a reaction kit (Applied Biosystems, Waltham, MA, USA). Quantitative analysis of target marker was performed with qRT-PCR using the relative standard curve method. TaqMan or SYBR green analysis was conducted by using an Applied Biosystems 7500 Sequence Detector (Applied Biosystems, Waltham, MA, USA). The expression levels were normalized to 18S rRNA. All primer sequences are provided in Table S2.

4.6. Kidney Histopathology

Histological kidney assessment was performed as previously reported [39]. Formalin-fixed, paraffin-embedded sections (2 μm) of kidneys were subjected to periodic acid–Schiff (PAS) and Sirius red (SR) staining. The PAS reaction visualized the basement membranes of the capillary loops of the glomeruli, through which the glomerular damage can be evaluated [7]. In each group, 10 fields of view were randomly selected from each kidney sample section under a 400 \times magnification, and the average ratio of glomerular section area to total area within the view was calculated using the software ImageJ. SR staining allows for a quantification of interstitial fibrosis. The severity of tubule interstitial fibrosis was graded from 0 to 3 according to the distribution of lesions: 0, no lesion; 1, less than 20%; 2, 20–50%; 3, more than 50% [40]. Semi-quantitative glomerular damage and renal fibrotic scoring were performed in a blinded manner at 400 \times magnification per sample. All measurements were repeated three times.

4.7. Immunofluorescence and Immunohistochemistry

We performed immunostaining as previously described [7,41]. Immunofluorescence or immunohistochemistry was performed on 3- μm ice-cold acetone-fixed cryosections of kidneys using the following primary antibodies: anti-fibronectin, anti-CD4, anti-F4/80, anti-ICAM-1, anti- α -SMA (AbD Serotec, Oxford, UK). For indirect immunostaining, non-specific binding sites were blocked with 10% normal donkey serum for 30 min. Then, sections were incubated with the primary antibody for 1 h at room temperature or overnight at 4 $^{\circ}\text{C}$. All incubations were performed in a humid chamber. For fluorescence visualization of bound primary antibodies, sections were further incubated with Cy3-conjugated secondary antibodies (Jackson Immuno Research, WG, USA) for 1 h in a humid chamber at room temperature. Slides were analyzed using a Zeiss Axioplan-2 imaging microscope with the computer program AxioVision 4.8 (Zeiss, Jena, Germany). For immunohistochemistry, after incubation with the primary antibody directed against α -SMA, biotinylated secondary antibody (Dako REALTM EnVisionTM; Dako Denmark A/S, Glostrup, Denmark) was used. Immunohistochemical positive staining was consecutively revealed by the 3,3'-Diaminobenzidine Peroxidase Substrate Kit (Dako REALTM EnVisionTM; Dako Denmark A/S, Glostrup, Denmark) in accordance with the manufacturer's instructions.

Quantitative analyses of infiltrating cells (CD4+ and F4/80+) and fibroblasts (α -SMA+) were counted in 15 non-overlapping, randomly chosen fields per kidney section under a 400 \times magnification. The average ratio of the fibronectin or ICAM-1-labeled area to the total area in the view (400 \times) was calculated using the software ImageJ (NIH, Bethesda, MD, USA). In addition, ICAM-1 expression was also analyzed using software ImageJ to calculate the mean gray value (integrated density to area).

4.8. Statistics

Statistical analysis was performed using GraphPad 5.04 software. Study groups were analyzed by two-way ANOVA using Sidak's multiple comparisons post hoc test. Data are presented as mean \pm SD. p values < 0.05 were considered statistically significant.

Supplementary Materials: The following are available online at: <https://www.mdpi.com/article/10.3390/ijms23126870/s1>.

Author Contributions: Conceptualization, M.G., D.T. and L.M.; Data curation, Z.Z.; Formal analysis, Z.Z. and Y.X.; Funding acquisition, M.S., B.N. and M.G.; Investigation, Z.Z. and Y.X.; Methodology, Z.Z., U.K., M.S., B.N. and M.-B.K.; Project administration, M.G., D.T. and L.M.; Resources, U.K., T.G., M.G. and L.M.; Software, Z.Z., D.T. and L.M.; Supervision, M.G., D.T. and L.M.; Validation, D.T. and L.M.; Writing—original draft, Z.Z.; Writing—review and editing, M.G., D.T. and L.M. All authors agree to be accountable for all aspects of the work in ensuring that questions related to the accuracy or integrity of any part of the work are appropriately investigated and resolved. All authors made substantial contributions to conception, design, drafting and completion of the article. All authors have read and agreed to the published version of the manuscript.

Funding: This work was supported by the Deutsche Forschungsgemeinschaft (DFG) to M.G. (GO766/18-2, GO 766/12-3, SFB 1365), B.N. (NU 53/12-2) and M.S. (TRR 152) and Werner Jackstädt-Stiftung.

Institutional Review Board Statement: The animal study protocol was approved by the Berlin Animal Review Board, Berlin, Germany and followed the restrictions in the Berlin State Office for Health and Social Affairs (Landesamt für Gesundheit und Soziales, LaGeSo) (license No. G0175/18, 11 Sep. 2018). All experiments were performed in accordance with ARRIVE guidelines.

Informed Consent Statement: Not applicable.

Data Availability Statement: Represented data are publicly archived datasets. For further information, please contact the corresponding author.

Acknowledgments: We thank Mario Kaßmann for his administrative support. We thank Jana Czychi, Gabriele N'diaye, and Juliane Ulrich for their technical help. We acknowledge financial support from the Open Access Publication Fund of Charité—Universitätsmedizin Berlin and the German Research Foundation (DFG).

Conflicts of Interest: The authors declare no conflict of interest.

References

1. Jha, V.; Garcia-Garcia, G.; Iseki, K.; Li, Z.; Naicker, S.; Plattner, B.; Saran, R.; Wang, A.Y.; Yang, C.W. Chronic kidney disease: Global dimension and perspectives. *Lancet* **2013**, *382*, 260–272. [[CrossRef](#)]
2. Genovese, G.; Friedman, D.J.; Ross, M.D.; Lecordier, L.; Uzureau, P.; Freedman, B.I.; Bowden, D.W.; Langefeld, C.D.; Oleksyk, T.K.; Uscinski Knob, A.L.; et al. Association of trypanolytic ApoL1 variants with kidney disease in African Americans. *Science* **2010**, *329*, 841–845. [[CrossRef](#)]
3. Li, X.; Pan, J.; Li, H.; Li, G. DsbA-L mediated renal tubulointerstitial fibrosis in UUO mice. *Nat. Commun.* **2020**, *11*, 4467. [[CrossRef](#)]
4. Black, L.; Lever, J.M.; Traylor, A.M.; Chen, B.; Yang, Z.; Esman, S.; Jiang, Y.; Cutter, G.; Boddu, R.; George, J.; et al. Divergent effects of AKI to CKD models on inflammation and fibrosis. *Am. J. Physiol. Ren. Physiol.* **2018**, *315*, F1107–F1118. [[CrossRef](#)]
5. Schlondorff, J. TRPC6 and kidney disease: Sclerosing more than just glomeruli? *Kidney Int.* **2017**, *91*, 773–775. [[CrossRef](#)] [[PubMed](#)]
6. Eddy, A.A. Overview of the cellular and molecular basis of kidney fibrosis. *Kidney Int Suppl (2011)*. **2014**, *4*, 2–8. [[CrossRef](#)] [[PubMed](#)]
7. Kong, W.; Haschler, T.N.; Nürnberg, B.; Krämer, S.; Gollasch, M.; Markó, L. Renal Fibrosis, Immune Cell Infiltration and Changes of TRPC Channel Expression after Unilateral Ureteral Obstruction in *Trpc6*^{-/-} Mice. *Cell Physiol. Biochem.* **2019**, *52*, 1484–1502. [[PubMed](#)]
8. Lin, B.L.; Matera, D.; Doerner, J.F.; Zheng, N.; Del Camino, D.; Mishra, S.; Bian, H.; Zeveleva, S.; Zhen, X.; Blair, N.T.; et al. In vivo selective inhibition of TRPC6 by antagonist BI 749327 ameliorates fibrosis and dysfunction in cardiac and renal disease. *Proc. Natl. Acad. Sci. USA* **2019**, *116*, 10156–10161. [[CrossRef](#)]
9. Ilatovskaya, D.V.; Staruschenko, A. TRPC6 channel as an emerging determinant of the podocyte injury susceptibility in kidney diseases. *Am. J. Physiol. Ren. Physiol.* **2015**, *309*, F393–F397. [[CrossRef](#)]
10. Dryer, S.E.; Roshanravan, H.; Kim, E.Y. TRPC channels: Regulation, dysregulation and contributions to chronic kidney disease. *Biochim. Biophys. Acta Mol. Basis Dis.* **2019**, *1865*, 1041–1066. [[CrossRef](#)]
11. Winn, M.P.; Conlon, P.J.; Lynn, K.L.; Farrington, M.K.; Creazzo, T.; Hawkins, A.F.; Daskalakis, N.; Kwan, S.Y.; Ebersviller, S.; Burchette, J.L.; et al. A mutation in the TRPC6 cation channel causes familial focal segmental glomerulosclerosis. *Science* **2005**, *308*, 1801–1804. [[CrossRef](#)] [[PubMed](#)]
12. Reiser, J.; Polu, K.R.; Moller, C.C.; Kenlan, P.; Altintas, M.M.; Wei, C.; Faul, C.; Herbert, S.; Villegas, I.; Avila-Casado, C.; et al. TRPC6 is a glomerular slit diaphragm-associated channel required for normal renal function. *Nat. Genet.* **2005**, *37*, 739–744. [[CrossRef](#)] [[PubMed](#)]
13. Riehle, M.; Buscher, A.K.; Gohlke, B.O.; Kassmann, M.; Kolatsi-Joannou, M.; Brasen, J.H.; Nagel, M.; Becker, J.U.; Winyard, P.; Hoyer, P.F.; et al. TRPC6 G757D Loss-of-Function Mutation Associates with FSGS. *J. Am. Soc. Nephrol.* **2016**, *27*, 2771–2783. [[CrossRef](#)] [[PubMed](#)]
14. Zheng, Z.; Tsvetkov, D.; Bartolomaeus, T.U.P.; Erdogan, C.; Krügel, U.; Schleifenbaum, J.; Schaefer, M.; Nürnberg, B.; Chai, X.; Ludwig, F.A.; et al. Role of TRPC6 in kidney damage after acute ischemic kidney injury. *Sci. Rep.* **2022**, *12*, 3038. [[CrossRef](#)] [[PubMed](#)]
15. Häfner, S.; Burg, F.; Kannler, M.; Urban, N.; Mayer, P.; Dietrich, A.; Trauner, D.; Broichhagen, J.; Schaefer, M. A (+)-Larixol Congener with High Affinity and Subtype Selectivity toward TRPC6. *ChemMedChem* **2018**, *13*, 1028–1035. [[CrossRef](#)] [[PubMed](#)]
16. Breyer, M.D.; Böttinger, E.; Brosius, F.C., 3rd; Coffman, T.M.; Harris, R.C.; Heilig, C.W.; Sharma, K. Mouse models of diabetic nephropathy. *J. Am. Soc. Nephrol.* **2005**, *16*, 27–45. [[CrossRef](#)]
17. Markó, L.; Park, J.K.; Henke, N.; Rong, S.; Balogh, A.; Klamer, S.; Bartolomaeus, H.; Wilck, N.; Ruland, J.; Forslund, S.K.; et al. B-cell lymphoma/leukaemia 10 and angiotensin II-induced kidney injury. *Cardiovasc. Res.* **2020**, *116*, 1059–1070. [[CrossRef](#)]

18. Chevalier, R.L.; Forbes, M.S.; Thornhill, B.A. Ureteral obstruction as a model of renal interstitial fibrosis and obstructive nephropathy. *Kidney Int.* **2009**, *75*, 1145–1152. [CrossRef]
19. Lv, W.; Booz, G.W.; Wang, Y.; Fan, F.; Roman, R.J. Inflammation and renal fibrosis: Recent developments on key signaling molecules as potential therapeutic targets. *Eur. J. Pharmacol.* **2018**, *820*, 65–76. [CrossRef]
20. Wu, Y.L.; Xie, J.; An, S.W.; Oliver, N.; Barrezueta, N.X.; Lin, M.H.; Birnbaumer, L.; Huang, C.L. Inhibition of TRPC6 channels ameliorates renal fibrosis and contributes to renal protection by soluble klotho. *Kidney Int.* **2017**, *91*, 830–841. [CrossRef] [PubMed]
21. LeBleu, V.S.; Taduri, G.; O'Connell, J.; Teng, Y.; Cooke, V.G.; Woda, C.; Sugimoto, H.; Kalluri, R. Origin and function of myofibroblasts in kidney fibrosis. *Nat. Med.* **2013**, *19*, 1047–1053. [CrossRef]
22. Zeisberg, E.M.; Potenta, S.E.; Sugimoto, H.; Zeisberg, M.; Kalluri, R. Fibroblasts in kidney fibrosis emerge via endothelial-to-mesenchymal transition. *J. Am. Soc. Nephrol.* **2008**, *19*, 2282–2287. [CrossRef] [PubMed]
23. Lu, Y.A.; Liao, C.T.; Raybould, R. Single-Nucleus RNA Sequencing Identifies New Classes of Proximal Tubular Epithelial Cells in Kidney Fibrosis. *J. Am. Soc. Nephrol.* **2021**, *32*, 2501–2516. [CrossRef] [PubMed]
24. Tomasek, J.J.; Gabbiani, G.; Hinz, B.; Chaponnier, C.; Brown, R.A. Myofibroblasts and mechano-regulation of connective tissue remodelling. *Nat. Rev. Mol. Cell Biol.* **2002**, *3*, 349–363. [CrossRef]
25. Shlipak, M.G.; Fried, L.F.; Crump, C.; Bleyer, A.J.; Manolio, T.A.; Tracy, R.P.; Furberg, C.D.; Psaty, B.M. Elevations of inflammatory and procoagulant biomarkers in elderly persons with renal insufficiency. *Circulation* **2003**, *107*, 87–92. [CrossRef]
26. Chen, Q.; Zhou, Y.; Zhou, L.; Fu, Z.; Yang, C.; Zhao, L.; Li, S.; Chen, Y.; Wu, Y.; Ling, Z.; et al. TRPC6-dependent Ca(2+) signaling mediates airway inflammation in response to oxidative stress via ERK pathway. *Cell Death Dis.* **2020**, *11*, 170. [CrossRef] [PubMed]
27. European Bioinformatics Institute (EMBL-EBI); SIB Swiss Institute of Bioinformatics (PIR). P.I.R. Universal Protein Resource (Uniprot). Available online: <http://www.uniprot.org/> (accessed on 17 March 2022).
28. Damann, N.; Owsianik, G.; Li, S.; Poll, C.; Nilius, B. The calcium-conducting ion channel transient receptor potential canonical 6 is involved in macrophage inflammatory protein-2-induced migration of mouse neutrophils. *Acta Physiol.* **2009**, *195*, 3–11. [CrossRef] [PubMed]
29. Lindemann, O.; Umlauf, D.; Frank, S.; Schimmelpfennig, S.; Bertrand, J.; Pap, T.; Hanley, P.J.; Fabian, A.; Dietrich, A.; Schwab, A. TRPC6 regulates CXCR2-mediated chemotaxis of murine neutrophils. *J. Immunol.* **2013**, *190*, 5496–5505. [CrossRef]
30. Carrillo, C.; Hichami, A.; Andreoletti, P.; Cherkaoui-Malki, M.; del Mar Cavia, M.; Abdoul-Azize, S.; Alonso-Torre, S.R.; Khan, N.A. Diacylglycerol-containing oleic acid induces increases in [Ca(2+)](i) via TRPC3/6 channels in human T-cells. *Biochim. Biophys. Acta* **2012**, *1821*, 618–626. [CrossRef]
31. Conway, B.R.; O'Sullivan, E.D. Kidney Single-Cell Atlas Reveals Myeloid Heterogeneity in Progression and Regression of Kidney Disease. *J. Am. Soc. Nephrol.* **2020**, *31*, 2833–2854. [CrossRef]
32. Davis, J.; Burr, A.R.; Davis, G.F.; Birnbaumer, L.; Molkentin, J.D. A TRPC6-dependent pathway for myofibroblast transdifferentiation and wound healing in vivo. *Dev. Cell* **2012**, *23*, 705–715. [CrossRef] [PubMed]
33. Agell, N.; Bachs, O.; Rocamora, N.; Villalonga, P. Modulation of the Ras/Raf/MEK/ERK pathway by Ca(2+), and calmodulin. *Cell Signal* **2002**, *14*, 649–654. [CrossRef]
34. Andrikopoulos, P.; Kieswich, J.; Pacheco, S.; Nadarajah, L.; Harwood, S.M.; O'Riordan, C.E.; Thiemermann, C.; Yaqoob, M.M. The MEK Inhibitor Trametinib Ameliorates Kidney Fibrosis by Suppressing ERK1/2 and mTORC1 Signaling. *J. Am. Soc. Nephrol.* **2019**, *30*, 33–49. [CrossRef] [PubMed]
35. Zeng, F.; Miyazawa, T.; Kloepfer, L.A.; Harris, R.C. ErbB4 deletion accelerates renal fibrosis following renal injury. *Am. J. Physiol. Ren. Physiol.* **2018**, *314*, F773–F787. [CrossRef] [PubMed]
36. Mirhashemi, F.; Scherneck, S.; Kluth, O.; Kaiser, D.; Vogel, H.; Kluge, R.; Schürmann, A.; Neschen, S.; Joost, H.G. Diet dependence of diabetes in the New Zealand Obese (NZO) mouse: Total fat, but not fat quality or sucrose accelerates and aggravates diabetes. *Exp. Clin. Endocrinol. Diabetes* **2011**, *119*, 167–171. [CrossRef]
37. Restrictions in the State Office for Health and Social Affairs (LAGeSo). Animal Welfare. Available online: <https://www.berlin.de/lageso/gesundheit/veterinaerwesen/tierschutz/> (accessed on 17 August 2021).
38. Kilkenny, C.; Browne, W.J.; Cuthill, I.C.; Emerson, M.; Altman, D.G. Improving bioscience research reporting: The ARRIVE guidelines for reporting animal research. *PLoS Biol.* **2010**, *8*, e1000412. [CrossRef]
39. Manna, M.; Markó, L.; Balogh, A.; Vigolo, E.; N'Diaye, G.; Kaßmann, M.; Michalick, L.; Weichelt, U.; Schmidt-Ott, K.M.; Liedtke, W.B.; et al. Transient Receptor Potential Vanilloid 4 Channel Deficiency Aggravates Tubular Damage after Acute Renal Ischaemia Reperfusion. *Sci. Rep.* **2018**, *8*, 4878. [CrossRef]
40. Zheng, Z.; Li, C.; Shao, G.; Li, J.; Xu, K.; Zhao, Z.; Zhang, Z.; Liu, J.; Wu, H. Hippo-YAP/MCP-1 mediated tubular maladaptive repair promote inflammation in renal failed recovery after ischemic AKI. *Cell Death Dis.* **2021**, *12*, 754. [CrossRef]
41. Zheng, Z.; Deng, G.; Qi, C.; Xu, Y.; Liu, X.; Zhao, Z.; Zhang, Z.; Chu, Y.; Wu, H.; Liu, J. Porous Se@SiO₂ nanospheres attenuate ischemia/reperfusion (I/R)-induced acute kidney injury (AKI) and inflammation by antioxidative stress. *Int. J. Nanomed.* **2019**, *14*, 215–229. [CrossRef]